In-Situ Characterization of Potential-Induced Degradation in Crystalline Silicon Photovoltaic Modules Through Dark *I–V* Measurements

Wei Luo, Peter Hacke, Jai Prakash Singh, Jing Chai, Yan Wang, Seeram Ramakrishna, Armin G. Aberle, and Yong Sheng Khoo

***Abstract*—A temperature correction methodology for *in-situ* dark *I–V* (DIV) characterization of conventional p-type crystalline silicon photovoltaic (PV) modules undergoing potential-induced degradation (PID) is proposed. We observe that the DIV-derived module power temperature coefficient (γ_{dark}) varies as a function of the extent of PID. To investigate the relationship between γ_{dark} and DIV-derived module power ($P_{\mathrm{dark}}(T_s)$, measured *in situ* and at the stress temperature) two parameters are defined: change in the DIV-derived module temperature coefficient ($\Delta\gamma_{\mathrm{dark}}$) and DIV-derived module power degradation at the PID stress temperature ($\Delta P_{\mathrm{dark}}(T_s)$). It is determined that there is a linear relationship between $\Delta\gamma_{\mathrm{dark}}$ and $\Delta P_{\mathrm{dark}}(T_s)$. Based on this finding, we can easily determine the module γ_{dark} at various stages of PID by monitoring $P_{\mathrm{dark}}(T_s)$ *in situ*. We then further develop a mathematical model to translate $P_{\mathrm{dark}}(T_s)$ to that at 25 °C ($P_{\mathrm{dark}}(25\,^{\circ}\mathrm{C})$), which is correlated with the module power measured at the standard testing conditions (P_{STC}). Our experiments demonstrate that, for various degrees of PID, the temperature correction methodology offers a relative accuracy of ±3% for predicting P_{STC}. Furthermore, it reduces the root-mean-square error (RMSE) by around 70%, compared with the P_{STC} estimation without the temperature correction.**

***Index Terms*—*In-situ* dark *I–V* (DIV) characterization, module power temperature coefficient, photovoltaic (PV) modules, potential-induced degradation (PID), temperature correction.**

I. Introduction

POTENTIAL-INDUCED degradation (PID) has received considerable attention in recent years due to the detrimental impact on photovoltaic (PV) module performance under field conditions. In conventional p-type crystalline silicon (c-Si) PV modules, PID shunting (PID-s) due to Na-decorated stacking faults across p-n junctions has been identified as the root cause [1]–[3]. To prevent PID in the field, PV modules are usually subjected to accelerated laboratory PID tests, during which samples are frequently removed from the climate chamber for light *I–V* (LIV) measurements to determine their power degradation at standard testing conditions (STC). This process requires considerable time and effort, particularly when a large number of PV modules are being evaluated. Dark *I–V* (DIV) characterization is a useful technique to monitor the module power performance *in situ* during the accelerated PID testing [4], [5]; it allows the measurements of module performance in greater detail for understanding the nature of the degradation [4], [5] and can be used to evaluate the module power in the climate chamber without taking the module offline for LIV measurements under STC [6], [7]. The method is simple to apply and enables researchers to intermittently determine power loss due to PID without interrupting the PID test. Therefore, significant time and cost can be saved for chamber-based PID tests.

The DIV characterization technique has been receiving growing interest from researchers considering its advantages. Based on the superposition principle [8], the DIV measurement at 25 °C has been successfully used to estimate the module power degradation at STC due to PID with a high degree of accuracy [9]–[11]. However, to accelerate the PID process, PV modules are often stressed at a temperature much higher than 25 °C (e.g., 50 or 60 °C). This temperature difference introduces substantial error to the prediction of module power under STC (P_{STC}) by the *in-situ* DIV measurement, if no correction step is applied, since the device performance is greatly affected by temperature. It is also not ideal to stop the test, ramp down the temperature to 25 °C to perform the DIV measurement, and ramp up to the stress temperature (T_s) to resume the test. Not only is this process time consuming, but it might also affect the test due to PID recovery [12], [13].

An error compensation method was proposed and implemented in [6] and [7] to improve the accuracy for predicting module power at STC (P_{STC}) with *in-situ* DIV measurements. In the present paper, we develop a fundamentally different approach focusing on the temperature correction, which is based on the DIV-derived module temperature coefficient γ_{dark} [6]. Temperature correction can be performed to translate the DIV-derived module power (P_{dark}) measured at a higher temperature

Manuscript received September 13, 2016; revised October 12, 2016; accepted October 17, 2016. The work at the Solar Energy Research Institute of Singapore was supported by the National University of Singapore (NUS) and the National Research Foundation of Singapore through the Singapore Economic Development Board. The work at the National Renewable Energy Laboratory (P. Hacke) was supported by the U.S. Department of Energy under Contract No. DE-AC36-08GO28308. Funding was provided by the SuNLaMP program of the Office of Energy Efficiency & Renewable Energy.

W. Luo and S. Ramakrishna are with the Solar Energy Research Institute of Singapore, Singapore 117574, and also with the Department of Mechanical Engineering, National University of Singapore, Singapore 117575 (e-mail: serlw@nus.edu.sg; seeram@nus.edu.sg).

P. Hacke is with the National Renewable Energy Laboratory, Golden, CO 80401 USA (e-mail: Peter.Hacke@nrel.gov).

J. P. Singh, J. Chai, Y. Wang, and Y. S. Khoo are with the Solar Energy Research Institute of Singapore, Singapore 117574 (e-mail: jaiprakash.singh@nus.edu.sg; chai.jing@nus.edu.sg; yan.wang@nus.edu.sg; yongshengkhoo@nus.edu.sg).

A. G. Aberle is with the Solar Energy Research Institute of Singapore, Singapore 117574, and also with the Department of Electrical and Computing Engineering National University of Singapore, Singapore 117583 (e-mail: armin.aberle@nus.edu.sg).

Color versions of one or more of the figures in this paper are available online at http://ieeexplore.ieee.org.

Digital Object Identifier 10.1109/JPHOTOV.2016.2621352

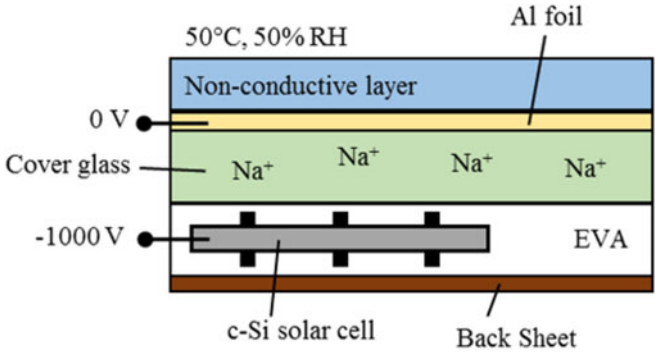

Fig. 1. Simplified schematic of the PID test setup inside a climate chamber. The minimodules being tested consist of four cells, but only one cell is shown in this figure for simplicity. The Al foil is pressed against the cover glass by the weight of the nonconductive layer.

to that at 25 °C (corresponding to STC), using the DIV-derived module γ_{dark}. However, it is reported that the absolute module power temperature coefficient decreases as PID progresses in conventional c-Si PV modules [14], as does the DIV-derived module γ_{dark} [6]. Therefore, it is not valid to use the DIV-derived module γ_{dark} before PID to correct the module P_{dark} to that at different temperatures (e.g., 25 °C) over the course of the PID evolution.

In this study, we devised systematic experiments to investigate the relationship between the 1) DIV-derived module γ_{dark} and 2) DIV-derived module power $P_{\mathrm{dark}}(T_s)$, measured *in situ* and at the stress temperature (T_s) over the course of PID progression in conventional p-type c-Si PV modules. Using the newly found relationship, we developed a mathematical model to translate the DIV-derived module $P_{\mathrm{dark}}(T_s)$ to that at 25 °C, which is correlated with module power under STC (P_{STC}).

II. Experimental Design

Accelerated PID tests were conducted on four frameless p-type c-Si minimodules (four cells) with the standard glass–EVA–cell–EVA–backsheet package, as shown in Fig. 1. During the tests, the temperature and relative humidity inside the climate chamber were maintained at 50 °C and 50% RH, respectively. The ramping process was optimized to avoid condensation and minimize the ramping time. A layer of aluminum (Al) foil was placed on top of the minimodules and was connected to the positive terminal of a high-voltage power source. The positive terminal of the power source was also grounded. A voltage of -1000 V was applied to the solar cells, by connecting the shorted leads to the negative terminal of the same power source. In order to maintain a uniform and consistent contact between the front glass surface and the Al foil, a layer of nonconductive material was placed on top of the Al foil.

The samples were intermittently removed from the climate chamber to perform LIV and DIV measurements at different temperatures with a class A+A+A+ HALM system. The light intensity was 1000 W/m^2 for all LIV measurements. The LIV and DIV measurements were performed immediately after removal of the samples from the chamber. After the measurements, the modules were immediately returned to the chamber to resume PID testing. In general, the samples were returned to the chamber within 3 h to minimize PID recovery. Four temperature sensors were attached to the rear surface of the minimodules for temperature measurements. *I–V* measurements were carried out only when the module temperature had stabilized to ensure that the cells had reached thermal equilibrium with the module package.

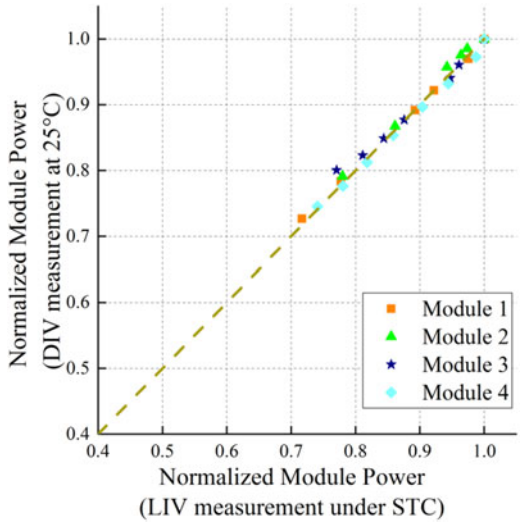

Fig. 2. Comparison of the normalized power measured by DIV at 25 °C and LIV at STC for four modules undergoing accelerated PID testing (–1000 V, 50 °C, 50% RH, Al foil). The dashed line represents $y = x$.

III. Experimental Results

A. Validation of the Module P_{STC} Prediction by the Dark I–V Measurement at 25 °C

It has previously been established by Hacke *et al*. that the DIV measurement at 25 °C can accurately estimate the module P_{STC} for conventional p-type c-Si modules undergoing PID [9]–[11]. Our experiments also demonstrated the same observations, as shown in Fig. 2, where the normalized module power measured by DIV at 25 °C and by LIV at STC are compared. As can be seen from Fig. 2, all points fall on or near the line $y = x$, validating the module P_{STC} prediction by the DIV measurement at 25 °C. The DIV-derived module power P_{dark} is evaluated by shifting the DIV curve by the photocurrent I_{ph}, according to the superposition principle. The I_{ph} is obtained from the LIV measurement at STC, which degrades insignificantly as PID progresses. The module power is normalized by dividing the measured module power at different time intervals with the module power measured prior to PID. The results indicate that during PID testing, if the normalized module P_{dark}(25 °C) is measured with DIV characterization, the normalized module P_{STC} can be approximated accurately. Therefore, P_{STC} can be predicted without LIV measurements under STC over the course of PID testing.

B. Dark I–V-Derived Module Power Temperature Coefficient

When the DIV curve is obtained at a higher temperature, temperature correction can be performed using the module's DIV-derived power temperature coefficient to translate the module

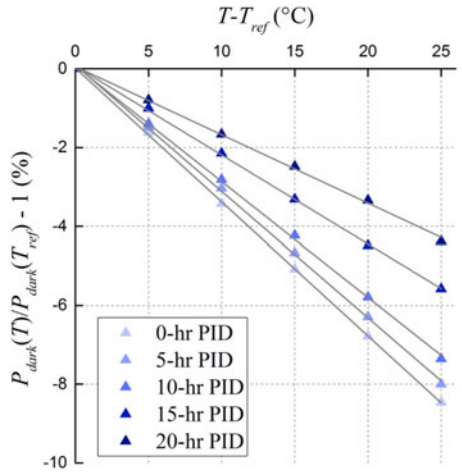

Fig. 3. Reduction of the DIV-derived module γ_{dark} for module 4 undergoing PID. The other three modules showed the same behavior. The slope of the lines represents the absolute value of the DIV-derived module γ_{dark}. The data are fitted by the linear regression method with the intercept set as 0.

power to that at 25 °C ($P_{\mathrm{dark}}(25^{\circ}\mathrm{C})$). The module $P_{\mathrm{dark}}(25\,^{\circ}\mathrm{C})$ can then be used to predict the module P_{STC}, as has been discussed in the previous section. According to [6], [15], and [16], the DIV-derived module power temperature coefficient (γ_{dark}) can be defined as follows:

$$\frac{P_{\mathrm{dark}}\,(T_c)}{P_{\mathrm{dark}}\,(T_{\mathrm{ref}})} = 1 + \gamma_{\mathrm{dark}}\,(T_c - T_{\mathrm{ref}}) \tag{1}$$

where $P_{\mathrm{dark}}(T_c)$ and $P_{\mathrm{dark}}(T_{\mathrm{ref}})$ represent the module power measured by DIV at T_c (cell temperature) and T_{ref} (reference temperature), respectively. In our experiments, the cell temperature is approximated to be the same as the module temperature, and the reference temperature is taken as 25 °C.

It is observed that the module γ_{dark} varies as a function of the extent of PID. As shown in Fig. 3, the absolute magnitude of the γ_{dark} for module 4 decreased as PID progressed. The steeper the slope, the greater the absolute magnitude of the module γ_{dark}. Before the PID stress, the module $\gamma_{\mathrm{dark}}(t = 0)$ was –0.339%/°C, and after 20 h of PID testing, it decreased to –0.170%/°C. Therefore, the module γ_{dark} measured before the PID testing cannot be used to correct the DIV-derived module power to that at 25 °C during PID testing, as it causes inaccuracy for the prediction of module P_{STC}. For example, if –0.339%/°C were used instead of –0.170%/°C after 20 h of PID ($T_s = 50^{\circ}\mathrm{C}$), a relative error of 4.23% would be induced in the temperature correction step. If the PID stress temperature were 60 °C, the relative error would increase to 5.92%.

C. Linear Relationship Between the Change in Dark I–V-Derived Module Temperature Coefficient and Power Degradation

To find the relationship between the temperature coefficient and module power degradation, two parameters are defined: change in the DIV-derived module temperature coefficient ($\Delta\gamma_{\mathrm{dark}}$) and DIV-derived module power degradation (ΔP_{dark}). The $\Delta\gamma_{\mathrm{dark}}$ and ΔP_{dark} are defined as follows:

$$\Delta\gamma_{\mathrm{dark}}\,(t) = 1 - \frac{\gamma_{\mathrm{dark}\,(t)}}{\gamma_{\mathrm{dark}\,(0)}} \tag{2}$$

$$\Delta P_{\mathrm{dark}}\,(T,t) = 1 - \frac{P_{\mathrm{dark}}\,(T,t)}{P_{\mathrm{dark}}\,(T,0)} \tag{3}$$

where $\gamma_{\mathrm{dark}}(0)$ and $\gamma_{\mathrm{dark}}(t)$ represent the DIV-derived module power temperature coefficient before PID and at the time interval *t*, respectively. $P_{\mathrm{dark}}(T,\,0)$ represents the DIV-derived module power, measured at temperature *T* and before PID. $P_{\mathrm{dark}}(T,\,t)$ represents the DIV-derived module power, measured at temperature *T* and at the time interval *t*.

During the PID testing, γ_{dark} is a function of stress time (*t*), and P_{dark} is a function of both the stress time and temperature. From Fig. 4, it is observed that there is an approximately linear relationship between $\Delta\gamma_{\mathrm{dark}}$ and ΔP_{dark}, measured at T_s of 50 °C for all four modules. Before PID testing ($t = 0$), there is no degradation for both the DIV-derived module γ_{dark} and P_{dark}; therefore, the first data point is always (0, 0). For this reason, the linear regression fitting was performed with the intercept set as 0. A statistical analysis was also performed to evaluate the linearity. The coefficient of determination, denoted as R^2, is a measure of the goodness-of-fit of the linear regression, with a value between 0 and 1. An R^2 of 1 indicates that the regression line perfectly fits the sample data. The R^2 value was computed for all four samples. They are 0.997, 0.996, 0.995, and 0.992 for modules 1–4, respectively. The R^2 results imply that the regression lines fit the experimental data exceptionally well. Therefore, it can be concluded that $\Delta\gamma_{\mathrm{dark}}(t)$ and $\Delta P_{\mathrm{dark}}(T_s, t)$ are linearly related.

The linear relationship also holds true for the other module temperatures. From Fig. 5, it can be seen that there is a linear relationship between the $\Delta\gamma_{\mathrm{dark}}$ and ΔP_{dark}, for module 1, where the module P_{dark} was measured at 25 and 45 °C, respectively. The R^2 value was computed for the regression lines for 25 and 45 °C, giving 0.998 and 0.997, respectively. The same calculations were repeated for modules 2–4 at different temperatures, and they all exhibited the same behavior. Therefore, it can be further concluded that $\Delta\gamma_{\mathrm{dark}}(t)$ and $\Delta P_{\mathrm{dark}}(T,t)$ are linearly related, independent of the module temperature at which the P_{dark} is measured. This finding has an important practical implication: the temperature correction method discussed in the current paper should be applicable for modules stressed at various temperatures.

IV. Temperature Correction for *In-Situ* Dark *I–V* Measurements

A. Theory

Based on the linear relationship, model (4) is proposed to predict the $\gamma_{\mathrm{dark}}\,(t)$ by the $P_{\mathrm{dark}}(T_s, t)$, at different time intervals

$$\left\{1 - \frac{\gamma_{\mathrm{dark}\,(t)}}{\gamma_{\mathrm{dark}\,(0)}}\right\} = k\left\{1 - \frac{P_{\mathrm{dark}}\,(T_s,t)}{P_{\mathrm{dark}}\,(T_s,0)}\right\} \tag{4}$$

where *k* represents the slope of the regression lines shown in Fig. 4. The *k* value varies for different modules and reflects different degradation paths.

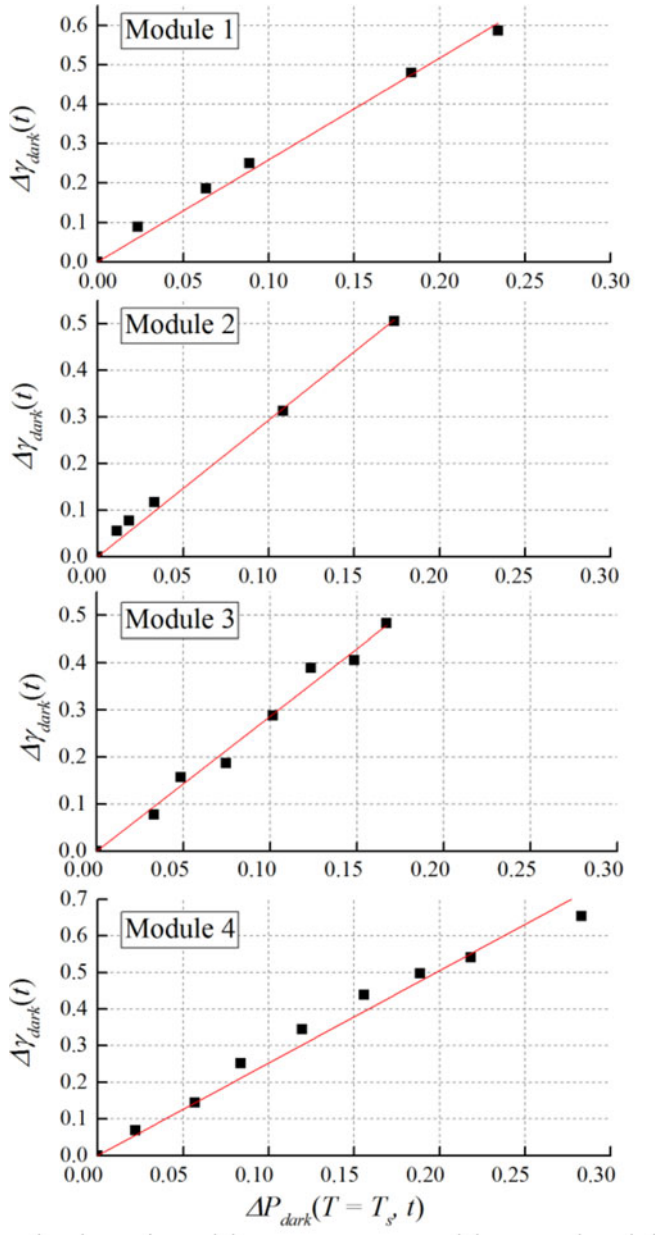

Fig. 4. Change in module γ_{dark} ($\Delta\gamma_{\mathrm{dark}}$) versus module power degradation (ΔP_{dark}) at $T_S = 50\,^{\circ}\mathrm{C}$ for all four samples. The initial γ_{dark} were –0.342%/°C, –0.334%/°C, –0.338%/°C, and –0.339%/°C for modules 1–4, respectively. The solid red lines are fitted by linear regression with the intercept set as 0.

In this model, $\gamma_{\mathrm{dark}}(0)$ and $P_{\mathrm{dark}}(T_s,\,0)$ are measured before PID testing. $P_{\mathrm{dark}}(T_s,\,t)$ can be determined with *in-situ* DIV measurements at different time intervals, for example, every 2 h. As for *k*, ideally, the PID testing should be stopped at several time intervals (t_1, t_2, t_3, etc.) to measure the module $\gamma_{\mathrm{dark}}(t)$ and $P_{\mathrm{dark}}(T_s,\,t)$. The results can then be used to calculate the *k* value by linear regression fitting. However, since the purpose is

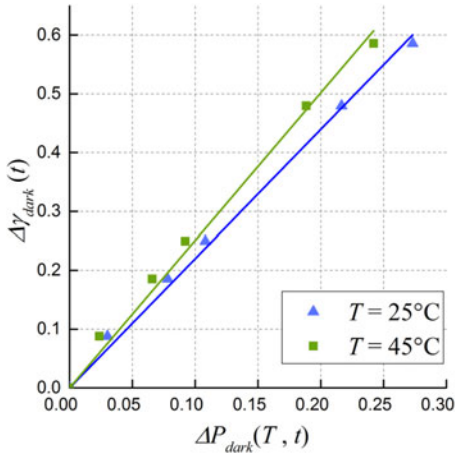

Fig. 5. Change in module γ_{dark} ($\Delta\gamma_{\mathrm{dark}}$) versus module power degradation (ΔP_{dark}) measured at different module temperatures for module 1; the lines are fitted by linear regression with the intercept set as 0.

to develop an *in-situ* characterization technique, the PID testing should not be interrupted. Therefore, we propose to estimate *k* with γ_{dark} and $P_{\mathrm{dark}}(T_s)$ measured before and after PID testing, using (5). The parameter t_n represents the time interval at the end of the PID test

$$k_{\mathrm{estimated}} = \left\{1 - \frac{\gamma_{\mathrm{dark}\,(t_n)}}{\gamma_{\mathrm{dark}\,(0)}}\right\} / \left\{1 - \frac{P_{\mathrm{dark}}\,(T_s, t_n)}{P_{\mathrm{dark}}\,(T_s, 0)}\right\}. \tag{5}$$

From (1), we can obtain

$$\frac{P_{\mathrm{dark}}\,(T_s, t)}{P_{\mathrm{dark}}\,(25\,^{\circ}\mathrm{C}, t)} = 1 + \gamma_{\mathrm{dark}}\,(t)\,(T_s - 25\,^{\circ}\mathrm{C}). \tag{6}$$

Combining (4) and (6), we obtain (7), shown at the bottom of the page.

As can be seen from (7), with $k_{\mathrm{estimated}}$, the $P_{\mathrm{dark}}(T_s,\,t)$, determined from *in-situ* DIV measurements at different time intervals, can be corrected to $P_{\mathrm{dark}}(25\,^{\circ}\mathrm{C}, t)$, which is correlated with P_{STC}. As discussed previously, $k_{\mathrm{estimated}}$ can be determined by *I–V* measurements before and after PID testing. Therefore, the module power P_{STC} can be determined *in situ* with the mathematical (7). The PID testing only has to be stopped for a few seconds for intermittent DIV sweeps of the sample module at the stress temperature, from which the PID degradation path can be calibrated at the end of the test. Therefore, not only does this characterization technique avoid the trouble due to LIV measurements, but it provides greater detail for understanding the nature of the degradation as well.

Additionally, to calculate $P_{\mathrm{dark}}(T_s,\,t)$ at different time intervals for DIV curves, the module I_{ph} at T_s has be to determined first. In this method, since LIV measurements are only conducted before and after PID testing, I_{ph} is approximated by the average of I_{ph} before and after PID testing and considered as constant throughout the PID testing. This is acceptable because

$$P_{\mathrm{dark}}\,(25\,^{\circ}\mathrm{C},\;\; t) = \frac{P_{\mathrm{dark}}\,(T_s,\;\; t)}{1 + \left\{1 - k_{\mathrm{estimated}}\left[1 - \frac{P_{\mathrm{dark}}(T_s,\;\; t)}{P_{\mathrm{dark}}(T_s,\;\; 0)}\right]\right\} * \gamma_{\mathrm{dark}}\,(0) * (T_s - 25)}. \tag{7}$$

TABLE I
DEGRADATION OF THE MODULE PHOTOCURRENT AT 50 °C AFTER PID TESTING FOR ALL FOUR MODULES

	Module 1	Module 2	Module 3	Module 4
$I_{\rm ph}$ at 50 °C before PID (A)	8.98	9.12	8.97	8.89
$I_{\rm ph}$ at 50 °C after PID (A)	8.83	9.03	8.87	8.77
$I_{\rm ph}$ degradation (%)	1.67	0.99	1.11	1.35

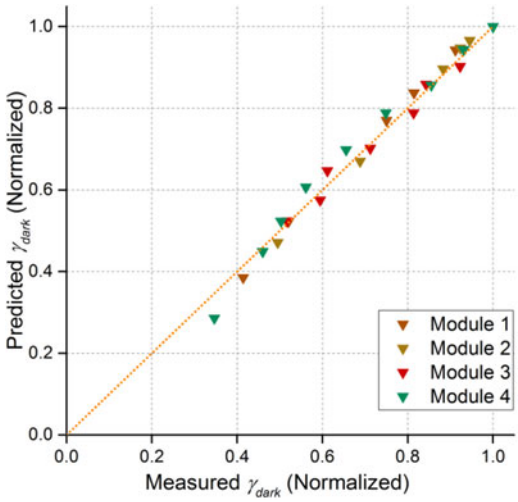

Fig. 6. Comparison of the predicted and the measured module $\gamma_{\rm dark}$ for all four modules. The module $\gamma_{\rm dark}$ is normalized. The dashed line represents $y = x$.

the change of $I_{\rm ph}$ is typically negligible for conventional c-Si PV modules undergoing PID testing. Our experiments revealed that the degradation of $I_{\rm ph}$ is less than 1.7% (see Table I), while the module $P_{\rm STC}$ degradation exceeds 20%.

B. Validation of the Prediction Model for Dark I–V-Derived Module Temperature Coefficient

With the estimated *k* from (5), $\gamma_{\rm dark}\,(t)$ can be predicted with $P_{\rm dark}(T_s, t)$, according to model (4). $P_{\rm dark}(T_s, t)$ is calculated from *in-situ* DIV curves at different time intervals. The predicted $\gamma_{\rm dark}(t)$ is compared with the measured $\gamma_{\rm dark}(t)$ for all four samples, as shown in Fig. 6. $\gamma_{\rm dark}$ at different time intervals is normalized by dividing it by the initial value (before PID). As can be seen from Fig. 6, all the data points are close to the $y = x$ line, showing an excellent agreement. Nevertheless, there is a slight difference between the predicted and the measured value. Considering the fact that only two measurements are conducted for the estimation of *k*, the small deviation from the true value is acceptable.

C. Validation of the Temperature Correction Method

With the predicted $\gamma_{\rm dark}(t)$ from model (4), the intermittently measured $P_{\rm dark}(T_s = 50\,^{\circ}{\rm C}, t)$ can be translated to $P_{\rm dark}(25^{\circ}{\rm C}, t)$, which estimates the $P_{\rm STC}$ with a high degree of accuracy. The normalized module power, measured by the LIV measurement under STC, is compared with the normalized module power at STC as predicted by the *in-situ* DIV measurement. As can been seen from Fig. 7, all the data points fall within the region sandwiched by the two red lines, which represent a relative prediction error of 3%. Therefore, it can be concluded that, after the temperature correction, *in-situ* DIV measurements at T_s can accurately predict the module power loss at STC due to PID.

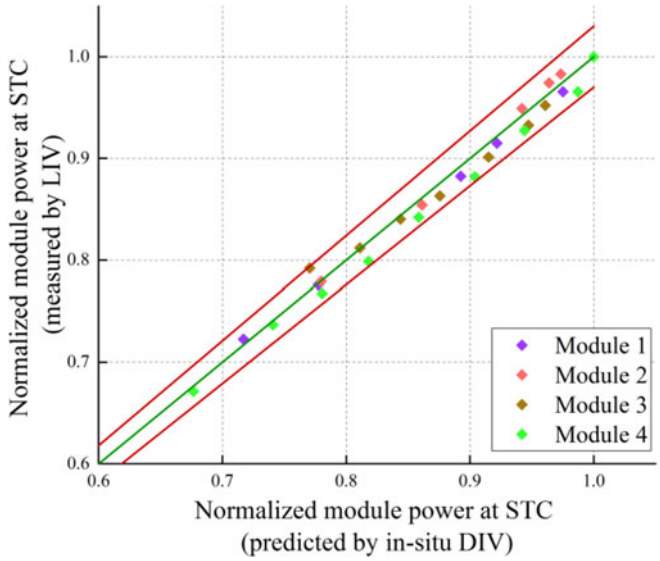

Fig. 7. Normalized PV module power at STC calculated from the *in-situ* DIV measurement at T_s versus normalized PV module power at STC by the LIV measurement. The top red line represents $y = 1.03x$. The bottom red line represents $y = 0.97x$. The green line represents $y = x$.

TABLE II
SUMMARY OF THE RMSE FOR THE SAMPLE DATA BEFORE AND AFTER THE TEMPERATURE CORRECTION

	Module 1	Module 2	Module 3	Module 4
$\rm RMSE_1$	0.037	0.031	0.035	0.032
$\rm RMSE_2$	0.007	0.007	0.012	0.015
Error reduction (%)	81.1	77.4	65.7	53.1

The root-mean-square error (RMSE) is also calculated for the sample data before and after the temperature correction, using (8). They are denoted as $\rm RMSE_1$ and $\rm RMSE_2$, respectively:

$$\text{RMSE} = \sqrt{\left\{\sum_{k=1}^{n}\left(P_{\rm STC,predicted} - P_{\rm STC,\,measured}\right)_{t_k}{}^2\right\}/n} \quad (8)$$

where t_1, t_2, t_3, ….., t_n represents the time interval when the modules were removed from the climate chamber for DIV and LIV measurements using the HALM system. The parameter *n* represents the number of intervals.

$P_{\rm STC,predicted}$ and $P_{\rm STC,measured}$ were normalized for the calculation of RMSE, which is a measure of the difference between the predicted value and the measured value. A larger RMSE value generally represents a greater difference between the estimated value and the true value. The RMSE results are summarized in Table II. As can be seen, after the correction, the RMSE can be reduced by an average of 69.3%. Therefore,

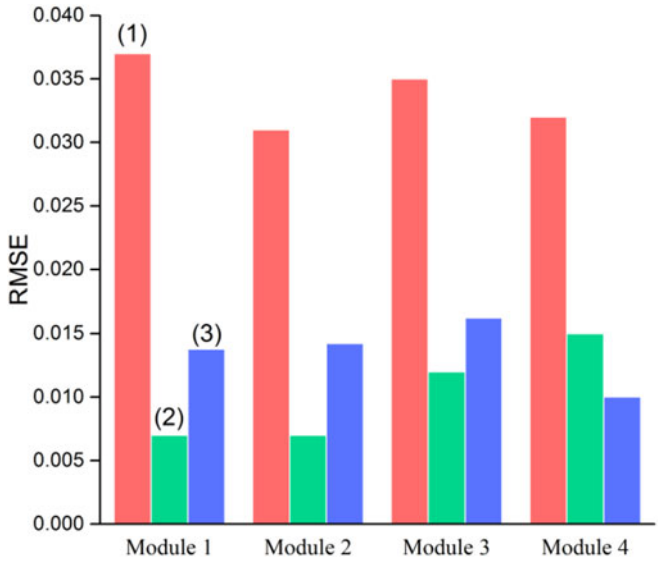

Fig. 8. Comparison of the RMSE of P_{STC} prediction for three different cases: 1) without any correction step; 2) temperature correction method; and 3) error compensation method.

the temperature correction method significantly improves the accuracy of *in-situ* DIV characterization.

D. Comparison With the Error Compensation Method

The error compensation method is also implemented to correct the $P_{\mathrm{dark}}(T_s = 50\,^{\circ}\mathrm{C}, t)$ to $P_{\mathrm{dark}}(25\,^{\circ}\mathrm{C}, t)$ for the sample data, which is then used to predict module P_{STC}. The RMSE value is calculated after the error compensation step (denoted as RMSE_3) and is compared with the RMSE_2. As shown in Fig. 8, the error compensation method and the temperature correction method produce comparable results. We thus recommend to apply both methods to the *in-situ* DIV measurements and use the average of the two predictions. This can reduce uncertainties in the estimation and improve the consistency of the results. Further studies will be carried out in the future to compare the two methods extensively with a larger sample size.

V. Conclusion

In this paper, we have verified that the DIV measurement at 25 °C is able to predict the module power at STC for conventional c-Si modules undergoing PID testing with a high degree of accuracy. We also found a linear relationship between the change in module γ_{dark} $(\Delta\gamma_{\mathrm{dark}})$ and the degradation of P_{dark} $(\Delta P_{\mathrm{dark}})$. This relationship is independent of the module temperature at which P_{dark} was measured. Using this relationship, we developed a temperature correction methodology for *in-situ* DIV measurements. After the correction step, the *in-situ* DIV measurement at T_s can predict the module power loss at STC during accelerated PID testing with a relative accuracy of $\pm 3\%$ for conventional c-Si PV modules. An error analysis was performed to compare the accuracy of the prediction before and after the temperature correction. We showed that our correction method can reduce the RMSE by around 70% on average. The temperature correction method was also compared to the error compensation method, and it was shown that the two methods produced comparable results. Further studies are to be conducted in the future to examine the performance of these two methods with a larger sample size. We recommend to apply both methods to the *in-situ* DIV characterization and use the average of the predictions to reduce uncertainties in the estimation and improve the consistency of the predictions.

References

[1] D. Lausch *et al.*, "Potential-induced degradation (PID): Introduction of a novel test approach and explanation of increased depletion region recombination," *IEEE J. Photovoltaics*, vol. 4, no. 3, pp. 834–840, May 2014.

[2] V. Naumann *et al.*, "The role of stacking faults for the formation of shunts during potential-induced degradation of crystalline Si solar cells," *Phys. Status Solidi (RRL)—Rapid Res. Lett.*, vol. 7, pp. 315–318, 2013.

[3] V. Naumann *et al.*, "Explanation of potential-induced degradation of the shunting type by Na decoration of stacking faults in Si solar cells," *Sol. Energy Mater. Sol. Cells*, vol. 120, pp. 383–389, 2014.

[4] S. Stecklum, C. Völker, C. Eckerle, and D. Philipp, "In situ monitoring of PV modules by means of dark IV measurements during accelerated aging tests," presented at the 31st Eur. Photovoltaic Solar Energy Conf. Exh., Hamburg, Germany, 2015.

[5] D. King, B. Hansen, J. Kratochvil, and M. Quintana, "Dark current-voltage measurements on photovoltaic modules as a diagnostic or manufacturing tool," in *Proc. 26th IEEE Photovoltaic Spec. Conf.*, Anaheim, CA, USA, 1997, pp. 1125–1128.

[6] S. Spataru *et al.*, "Temperature-dependency analysis and correction methods of in situ power-loss estimation for crystalline silicon modules undergoing potential-induced degradation stress testing," *Prog. Photovoltaics, Res. Appl.*, vol. 23, pp. 1536–1549, 2015.

[7] P. Hacke and S. Spataru, "Automated data collection for determining statistical distributions of module power undergoing potential-induced degradation," in *Proc. 24th Workshop Crystalline Silicon Sol. Cells Modules: Mater. Processes*, Breckenridge, CO, USA, 2014. [Online]. Available: http://www.nrel.gov/docs/fy14osti/62468.pdf

[8] F. A. Lindholm, J. G. Fossum, and E. L. Burgess, "Application of the superposition principle to solar-cell analysis," *IEEE Trans. Electron Devices*, vol. ED-26, no. 3, pp. 165–171, Mar. 1979.

[9] P. Hacke *et al.*, "Testing and analysis for lifetime prediction of crystalline silicon PV modules undergoing degradation by system voltage stress," *IEEE J. Photovoltaics*, vol. 3, no. 1, pp. 246–253, Jan. 2013.

[10] P. Hacke *et al.*, "Acceleration factor determination for potential-induced degradation in crystalline silicon PV modules," in *Proc. IEEE Int. Rel. Phys. Symp.*, Anaheim, CA, USA, 2013, pp. 4B.1.1–4B.1.5.

[11] P. Hacke, K. Terwilliger, and S. Kurtz, "In-situ measurement of crystalline silicon modules undergoing potential-induced degradation in damp heat stress testing for estimation of low-light power performance," in *Proc. 23rd Workshop Crystalline Silicon Sol. Cells Modules: Mater. Processes*, Breckenridge, CO, USA, 2013. [Onine]. Available: http://www.nrel.gov/docs/fy13osti/60044.pdf

[12] D. Lausch *et al.*, "Sodium outdiffusion from stacking faults as root cause for the recovery process of potential-induced degradation (PID)," *Energy Procedia*, vol. 55, pp. 486–493, 2014.

[13] S. Pingel *et al.*, "Potential induced degradation of solar cells and panels," in *Proc. 35th IEEE Photovoltaic Spec. Conf.*, Honolulu, HI, USA, 2010, pp. 2817–2822.

[14] R. Desharnais, "Characterizing the impact of potential-induced degradation and recovery on the irradiance and temperature dependence of photovoltaic modules," in *Proc. 29th Eur. PV Sol. Energy Conf. Exhib.*, Amsterdam, The Netherlands, 2014, pp. 2346–2350.

[15] A. Parretta, A. Sarno, and L. R. Vicari, "Effects of solar irradiation conditions on the outdoor performance of photovoltaic modules," *Opt. Commun.*, vol. 153, pp. 153–163, 1998.

[16] C. R. Osterwald, "Translation of device performance measurements to reference conditions," *Sol. Cells*, vol. 18, pp. 269–279, 1986.

Authors' photographs and biographies not available at the time of publication.